Bulletin of Glacier Research 10 (1992) 69–74

Radio-echo sounding of Tyndall Glacier, southern Patagonia

Gino CASASSA
Byrd Polar Research Center and Department of Geological Sciences, The Ohio State University, Columbus, Ohio 43210 U.S.A.

(Received December 12, 1991 ; Revised manuscript received January 28, 1992)

Abstract

The first radar sounding measurements through glacier ice in Patagonia are reported. These measurements were carried out in December 1990 on Tyndall Glacier, an 8 km-wide temperate glacier on the Southern Patagonia Icefield. Two similar versions of an impulse radar designed to penetrate temperate ice were used. Ice thickness was measured successfully at seven sites across a transverse profile in the ablation area. A parabolic profile of the glacier bed was obtained, with a maximum thickness of 616 m at station T7, located 3 km from the left margin. No bottom reflection could be observed beyond station T7. We conclude that the large thickness of temperate ice of Tyndall Glacier exceeds the dynamic range of the radar.

1. Introduction

The Southern Patagonia Icefield (SPI) has an area of 13000 km^2 (Naruse and Aniya, 1992) and ranks as the largest temperate glacier of the southern hemisphere (Fig. 1). In spite of its large extent and importance as a sensitive indicator of the climatic change, it has been poorly studied in the past.

An extensive data set has been obtained for the Northern Patagonia Icefield (NPI) by the Glaciological Research Project in Patagonia (GRPP) through ground and aerial surveys carried out during 1983 to 1986 (Nakajima, 1985 ; 1987). The NPI is located 100 km north of the SPI and has an area of 4200 km^2 (Aniya, 1988). One of the main results of GRPP was that most of the outlet glaciers in the NPI have been thinning and retreating strongly in the past few decades (Aniya and Enomoto, 1986; Aniya, 1988). This prompted us to start in 1990 a project to study the extent and causes for ongoing variations of glaciers in the Southern Patagonia Icefield as a possible response to climatic changes (Naruse and Aniya, 1992).

The GRPP project included gravity surveys on Soler Glacier, Nef Glacier and the icefield. From these gravity data ice thickness values in excess of 1000 m were obtained (Casassa, 1987). However the poor accuracy of this technique was recognized as a serious limitation for glaciological studies. The 1990 project to study glacier variations provided a good opportunity to measure ice thickness with the more accurate ice radar technique. The selected site was Tyndall Glacier, located on the southeastern edge of the Southern Patagonia Icefield (Fig. 1).

2. Ice radar

Patagonian glaciers are temperate and have abundant meltwater. Therefore, a radar designed to penetrate temperate ice is necessary. Water inclusions within the ice produce a large scattering of radio waves. Based on scattering theory, Watts and England (1976) suggested criteria for designing an ice radar for temperate ice. They found that scattering is greatly reduced at frequencies below 10 MHz (30 m wavelength in air) which is much greater than their predicted size of the scattering inclusions (1 m). The first radar for temperate ice was developed by Vickers and Bollen (1974) under contract to the U.S. Geological Survey (USGS) and was tested successfully at South Cascade Glacier, Washington, and Columbia Glacier, Alaska.

Two radars that follow the USGS design were used. One is constructed at The Ohio State University (OSU), USA, and consists of a 12 V power unit and a transmitter built in the same box. The other radar is built at St. Olav College (STOC), Minnesota, USA, and consists of a separate 30 V power unit and a transmitter. Both produce a short-pulse voltage step

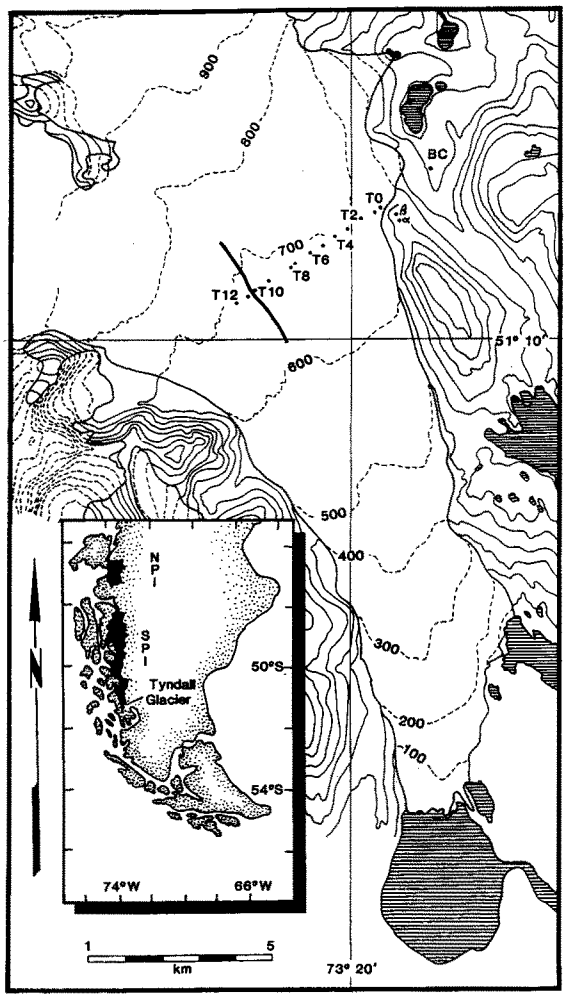

Fig. 1. Map of Tyndall Glacier (source : 1 : 100,000 scale map Parque Nacional Torres del Paine, Sociedad Turística Kaoniken Ltda. 1990. α and β are ground control points. Radar soundings were carried out at stations T1 to T12, but bottom reflections were only obtained up to station T7. The line at station T10 represents the medial moraine.

of a few hundred volts in amplitude which is radiated by a resistively loaded dipole antenna. The receiver consists of an identical antenna coupled to an oscilloscope from which data were captured with a standard photographic camera.

The OSU radar has been used extensively for determining bottom topography of tropical glaciers of Peru and China (Thompson *et al.*, 1982 ; 1988). The STOC radar has been used to study the water cavities in Variegated Glacier, Alaska (Jacobel and Anderson, 1987), and has also been tested in Ice Stream B, Antarctica (Jacobel *et al.*, 1988).

3. Sounding technique

A typical experiment consisted of laying the transmitting and receiving antennas on the ice parallel to glacier flow. Antenna separation was 45 m. A few times the antennas had to be laid over water -filled crevasses. The oscilloscope was coupled to the receiving antenna through a balun.

One person operated the transmitter, switching it on for a short period, while another person recorded the waveform at the oscilloscope with a standard photographic camera. The oscilloscope was a Hitachi V-209 and a simple mount was used for taking pictures. Taking pictures was not an easy task due to the high reflectivity of the glacier surface.

Dipole half-lengths (l) of 20 m and 40 m were used to evaluate the performance of different antennas. The center frequency (f) in MHz of the transmitted signal is given by the following empirical expression (Hodge, 1978) :

$$f=50/l. \quad (1)$$

This results in frequencies of 2.5 and 1.25 MHz for the half-dipole lengths of 20 and 40 m respectively.

4. Results

Radar soundings were carried out on twelve stations along a transverse profile on Tyndall Glacier. They are stations T1 to T12 in Fig. 1 and correspond to the survey stations measured by Kadota *et al.* (1992).

A standard radar waveform is shown in Fig. 2, which was recorded with the OSU radar at Guliya Ice Cap, China (Thompson, personal communication). Both the surface (S) and reflected (R) waves are clearly seen in Fig. 2. The surface wave is ideally a single (monopulse) wave (peaks 1 and 2), but in practice a second attenuated surface wave also appears (peaks 3 and 4). However, due to a lack of delay time of the oscilloscope used at Tyndall Glacier, the main part of the surface wave was lost in all the data. A typical waveform recorded at station T2 on Tyndall Glacier is shown in Fig. 3. In order to account for the zero-time uncertainty introduced by the oscilloscope delay time, our data were compared to the complete waveform of Fig. 2. Peaks 3 and 4 of the surface wave of Fig. 2 appear to correspond to peaks 3 and 4 of Fig. 3. Since the time between peaks 3 and 4 of the Guliya and Tyndall surface waves is very similar, the

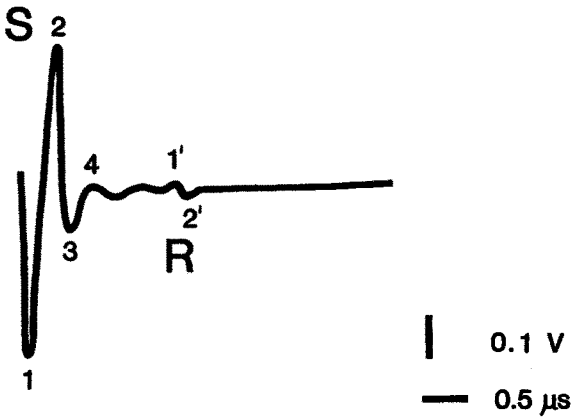

Fig. 2. Waveform recorded at Site 563 at 6200 m on Guliya Ice Cap, China (Lonnie Thompson, personal communication). S denotes the surface wave and R the reflected wave. Peaks 1 and 2 of the surface wave correspond to peaks 1' and 2' of the reflected wave.

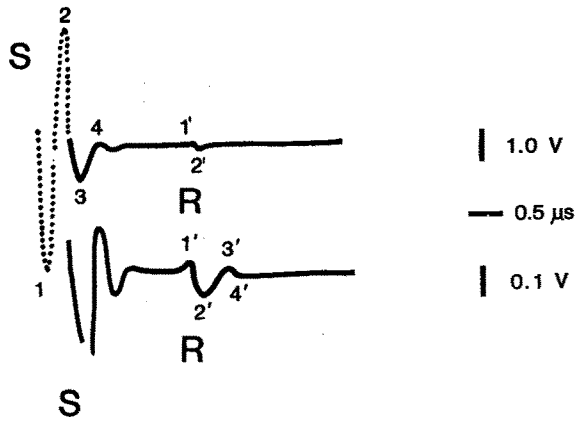

Fig. 3. Waveform recorded at station T2 with the OSU-2 radar. The timescale for the upper and lower waveforms is identical. The only difference is that the upper waveform is amplified 10 times in the lower waveform. The dotted line is the surface wave that has been reconstructed from Fig. 2. Numbers indicate corresponding peaks indicated on Fig. 2. Peak 4' practically cannot be distinguished in this particular waveform. A value of 0.4 μs is obtained for the interval between the zero time and the third peak (3) of the surface wave. The travel time t is measured from peak 1 to peak 1', peak 2 to peak 2', and so on for peaks 3 and 4.

Tyndall surface wave was reconstructed by assuming identical surface waves in both records. Travel times (t) of the wave reflected at the bed were computed as the time interval between the peaks of the reconstructed surface wave and corresponding peaks of the reflected wave, as shown in Fig. 3.

The following expression was used for computing ice thickness (Watts and Isherwood, 1978) :

$$D=\sqrt{\left(t+\frac{s}{c}\right)^2\frac{c^2}{4\epsilon_i}-\frac{s^2}{4}}, \qquad (2)$$

where c is the speed of light in vacuum (3×10^8 m/s), ε_i is the dielectric permittivity of ice (3.17), s is the separation distance between the transmitting and receiving antennas (45 m), and D is the ice thickness assuming a plane-layered geometry.

Table 1 summarizes the different radar measurements performed at each station. The coordinates and elevations of the stations are from Kadota *et al.* (1992). The radar model and antenna half-length are indicated. A travel time t is measured for each reflected peak as explained above. Ice thickness is calculated from the travel times using equation (2).

Reflections were strong and clear for stations T1, T2 and T3, with amplitudes ranging from 75 mV to 20 mV (Table 1). The reflections weakened substantially for station T4, where the amplitude was 5 mV. At station T7 the reflection had an amplitude of 2 mV, which is barely larger than the noise level (Figs. 4a and 4b). Beyond station T7 no reflection could be observed.

As is the case with the surface wave, the reflected wave consists in general of two waves of decaying amplitude. In half of the measurements the amplitude of the second wave (peaks 3' and 4' in Fig. 3) is comparable to that of the first wave (peaks 1' and 2' in Fig. 3). These waveforms will be named double reflections, as opposed to single reflections, *i.e.* where the amplitude of the second reflected wave is negligible. For double reflections, travel time was computed for both peaks of the first and second reflected waves, obtaining in total four travel times. Travel times are expressed as a time interval in Table 1 and as error bars of ice thickness in Fig. 5. The maximum ice thickness obtained is 582 to 616 m at station T7. As can be seen in Figs. 4a and 4b, the signal-to-noise level of the reflected wave at T7 is very close to 1, especially for the reflection of the STOC radar.

Unsuccessful radar measurements were carried out at stations T8 to T12. Several antenna orientations were tried, as well as two different antenna lengths, but no bottom reflection was observed. The near-parabolic profile of Fig. 5 suggests increased thicknesses beyond station T7. These large thicknesses probably attenuate the bottom reflection to

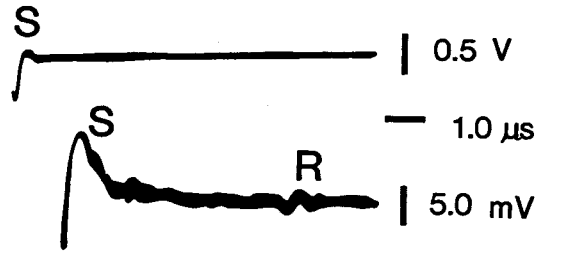

Fig. 4a. Waveform obtained at station T7 with the OSU-1 radar.

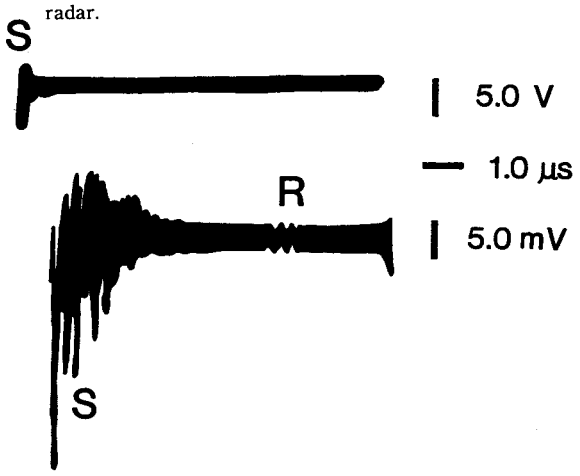

Fig. 4b. Waveform obtained at station T7 with the STOC radar. R is interpreted to be the bottom reflection. The timescale for the upper and lower waveforms is identical, the only difference being the amplitude scale.

such extent that it cannot be detected with the radar system used.

5. Discussion

A single reflection suggests a smooth bed. A double reflection suggests either a rough bed or scattering above the ice-bed interface. Half of the data show a double reflection. If this double reflection is indeed due to the roughness of the bed or scattering above the bed, we would also expect a double reflection when performing repeated soundings at the same site with a different radar or antenna length. In fact, at stations T2 and T7 both single and double reflections were obtained during repeated measurements. At T7 this is not meaningful due to the very low signal-to-noise level. But at T2 the signal-to-noise ratio is quite large, which suggests that the different reflected waves obtained are related to slight changes in the antenna orientation when performing a new measurement. This high sensitivity of the reflected wave could be due to large changes in bed roughness and scattering above the ice-bed interface at small spatial scale.

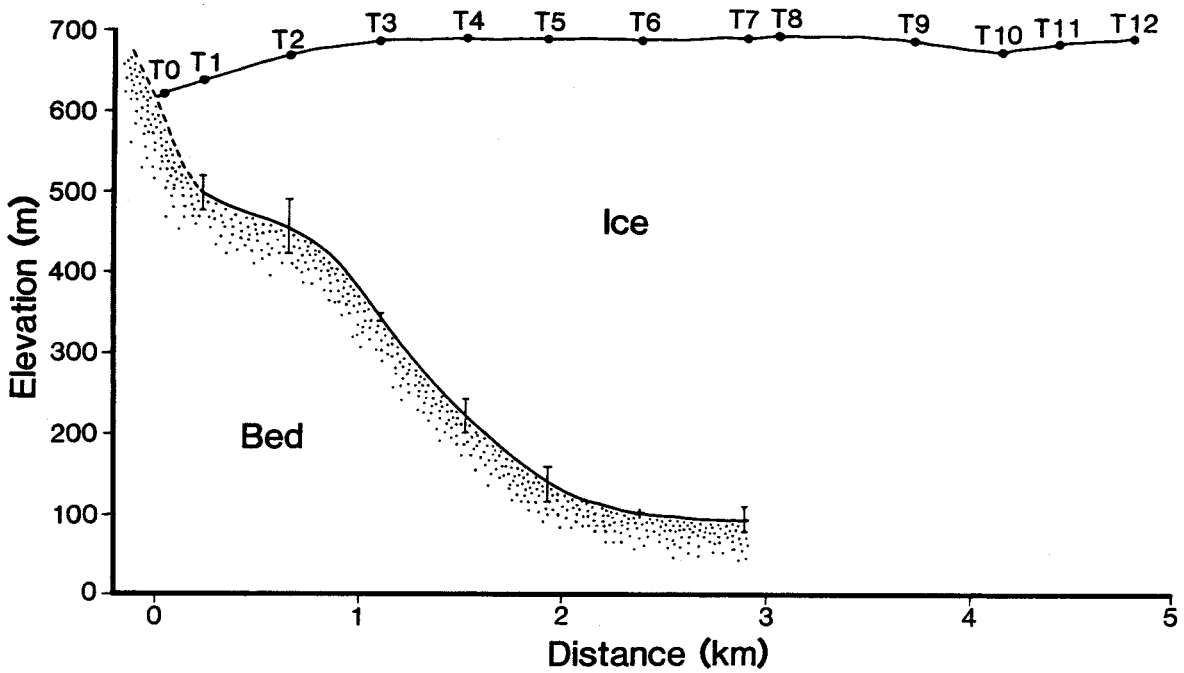

Fig. 5. Cross section of Tyndall Glacier. Close to the margin the bed has been extrapolated with a dashed line.

The phase shift between the surface wave and the reflected wave for a typical glacier bed is expected to be 180° because rock is a very good conductor compared to the highly resistive ice. However, most of the phase shift values shown in Table 1 are 0°. Jezek and Thompson (1982) report a near-zero phase shift value for Peruvian glaciers. They obtained a near-zero phase shift for a particular type of tuff using a two-layer and a three-layer model including air and water. At station T2 phase shifts of 0° and 180° are obtained. Again, this could indicate large variations in conditions at the bed at small spatial scale.

Antennas having dipole half-lengths of 20 and 40 m were used at station T2. No significant difference in travel time or reflected amplitude was obtained. The similar values of reflected amplitudes suggest no significant change in attenuation between wavelengths of 2.5 and 1.25 MHz.

The OSU radar performed slightly better than the STOC radar in deeper ice. At station 7 the reflected wave amplitude of the STOC radar (Fig. 4b) is the same as the noise level, whereas the OSU wave amplitude (Fig. 4a) is slightly larger than the noise level.

A parabolic increase in thickness and rapid decrease in reflected wave amplitude are observed toward the center of the glacier, and the reflected wave disappeared completely at station T8. This suggests that the electromagnetic wave is attenuated almost completely with ice thicknesses in excess of 600 m for the two radars used. However, ice thicknesses up to 1000 m have been recorded with a similar ground-based radar at Columbia Glacier, Alaska (Watts and Wright, 1981). This suggests that at Tyndall Glacier there is more attenuation, absorption or scattering of radio waves compared to Columbia Glacier.

One way of increasing the dynamic range of the radar is to increase the transmitting power. Another easier solution is to use a digital storage oscilloscope and stack several waveforms to increase the signal-to-noise level. This technique is being planned for the second phase of this field project.

Acknowledgments

Frank Huffman constructed the OSU radar, provided the oscilloscope and helped constantly throughout the project. Dr. Robert Jacobel provided the

Table 1

ST	DIST.	RADAR	ANT. LENGTH	PHASE SHIFT	AMPLI-TUDE	TIME		THICKNESS	
						PEAK 1 -PEAK 3	PEAK 2 -PEAK 4	PEAK 1 -PEAK 3	PEAK 2 -PEAK 4
	m		m	deg.	mV	μs	μs	m	m
T1	240	OSU-1	20	0	75	1.3-1.7	1.4-1.8	119-153	128-162
T2	654	OSU-1	20	0	75	2.4-2.8	2.4-2.7	213-246	213-238
T2	654	OSU-1	40	180	60	2.2	2.2	196	196
T2	654	OSU-2	40	180	75	2.0-2.5	1.8-2.3	179-221	162-204
T2	654	STOC	40	0	40	2.3	2.3	204	204
T3	1100	OSU-1	40	0	20	4.0	3.9	339	347
T4	1520	OSU-1	40	0	5	5.2-5.7	5.2-5.7	448-490	448-490
T5	1930	OSU-1	40	0	4	6.2-6.7	6.2-6.6	532-574	532-566
T6	2376	OSU-1	40	0	3	6.9	6.9	591	591
T7	2890	OSU-1	40	0	2	7.1	7.2	608	616
T7	2890	STOC	20	180	2	6.8-7.1	7.0-7.2	582-608	599-616

Notes: Distances are measured from the left margin of Tyndall Glacier. OSU-1 and OSU-2 are two identical models of the Ohio State University radar. STOC is the St. Olav College radar. Antenna lengths represent half-dipole lengths. For a single reflection, travel times are measured between corresponding peaks 1 and 1′ (PEAK 1) and peak 2 and 2′ (PEAK 2), and similarly for peaks 3, 3′ and 4, 4′, of the surface and reflected waves respectively. When a double reflection appears on the waveform, travel times are computed between corresponding and the reflected wave respectively and t is expressed as a range. The only exception is at station T1, where the range in time and thickness represents an uncertainty due to poor correlation of the surface and reflected wave peaks. Ice thickness was computed using eq. 2.

STOC radar and the antennas, giving valuable advice. The study was funded by the grant of International Scientific Program (No. 02041004 : led by R. Naruse) of the Ministry of Education, Science and Culture of Japan. The author acknowledges support from a grant of the Friends of Orton Hall Fund, Department of Geological Sciences, The Ohio State University. In the field the help and advice of Pedro Skvarca is greatly appreciated, as well as the assistance of Tsutomu Kadota and Rodrigo Gutiérrez. Mr. John Nagy of the Byrd Polar Research Center drafted the figures. This parer is Contribution 791 of the Byrd Polar Research Center, The Ohio State University.

References

1. Aniya, M. (1988) : Glacier inventory for the Northern Patagonia Icefield, Chile, and variations 1944/45 to 1985/86. Arctic and Alpine Research, **20** (2), 179−187.
2. Aniya, M. and Enomoto, H. (1986) : Glacier variations and their causes in the Northern Patagonia Icefield, Chile, since 1944. Arctic and Alpine Research, **18** (3), 307−316.
3. Casassa, G. (1987) : Ice thickness deduced from gravity anomalies on Soler Glacier, Nef Glacier and the Northern Patagonia Icefield. Bulletin of Glacier Research, **4**, 43−57.
4. Hodge, S. M. (1978) : USGS mono-pulse radar. Report, 1978, 9 p, unpublished.
5. Jacobel, R. W. and Anderson, S. K. (1987) : Interpretation of radio-echo returns from internal water bodies in Variegated Glacier, Alaska, USA. Journal of Glaciology, **33** (115), 319−323.
6. Jacobel, R. W., Anderson, S. K. and Rioux, D. F. (1988) : A portable digital data-acquisition system for surface-based ice-radar studies. Journal of Glaciology, **34** (118), 349−354.
7. Jezek, K. C. and Thompson, L. G. (1982) : Interpretation of mono-pulse ice radar soundings on two Peruvian Glaciers. IEEE Transactions on Geoscience and Remote Sensing, **GE -20** (3), 243−249.
8. Kadota, T., Naruse, R., Skvarca, P. and Aniya, M. (1992) : Ice flow and surface lowering of Tyndall Glacier, southern Patagonia. Bulletin of Glacier Research, **10**, 63−68.
9. Nakajima, C. (*Ed.*). (1985) : Glaciological Studies in Patagonia Northern Icefield, 1983−1984. Data Center for Glacier Research, Japanese Society of Snow and Ice, **2**, 133 p.
10. Nakajima, C. (1987) : Outline of the Glaciological Research Project in Patagonia, 1985−1986. Bulletin of Glacier Research, **4**, 1−6.
11. Naruse, R. and Aniya, M. (1992) : Outline of Glacier Research Project in Patagonia, 1990. Bulletin of Glacier Research, **10**, 31−38.
12. Thompson, L. G., Bolzan, J. F., Brecher, H. H., Kruss, P. D., Mosley-Thompson, E. and Jezek, K. C. (1982) : Geophysical investigations of the tropical Quelccaya Ice Cap, Peru. Journal of Glaciology, **28** (98), 57−69.
13. Thompson, L. G., Xiaoling, W., Mosley-Thompson, E. and Zichu, X. (1988) : Climatic records from the Dunde Ice Cap, China. Annals of Glaciology, **10**, 178−182.
14. Vickers, R. S. and Bollen, R. (1974) : An experiment in the radio echo sounding of temperate glaciers. Menlo Park, Calif., Stanford Research Institute, Final Report, 16 p, unpublished.
15. Watts, R. D. and England, A. W. (1976) : Radio-echo sounding of temperate glaciers : ice properties and sounder design criteria. Journal of Glaciology, **17** (75), 39−48.
16. Watts, R. D. and Isherwood, W. (1978) : Gravity surveys in glacier-covered regions. Geophysics, **43** (4), 819−822.
17. Watts, R. D. and Wright, D. L. (1981) : System for measuring thickness of temperate and polar ice from the ground or from the air. Journal of Glaciology, **27** (97), 459−469.